Supporting Information

Cheung et al. 10.1073/pnas.1008527107

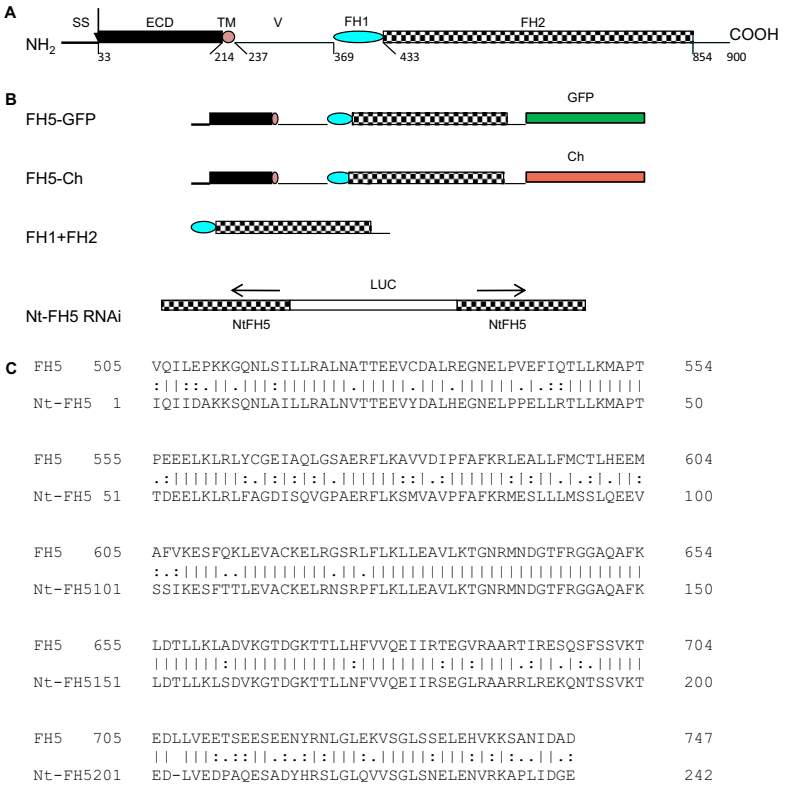

Fig. S1. FH5 domain map and transgenes. (*A*) A deduced protein domain map for FH5 (At5g54650). ECD, extracellular domain; SS, signal sequence; TM, transmembrane domain; V, variable domain; FH1, FH2, formin homology domain1 and -2. Numbers indicate the first amino acid residue in each of the domains. The cytoplasmic domain structure is conserved among formins (1). The N-terminal extension is unique to group I plant formins. (*B*) FH5-related transgene constructs. Transgenes were expressed from the popularly used pollen-expressed Lat52 promoter (2), except when the FH5 promoter (FH5p) (containing ~1.6 kbp DNA upstream of the annotated transcription start site) was used. For Nt-FH5 RNAi, a 729 base-pair region close to the C-terminal coding region of Nt-FH5 (see *C*) was divergently cloned, using the luciferase's (LUC's) coding sequence as stuffer. The same sequence was used for a Nt-FH5 antisense construct. Other transgenes used included Lat52::GFP-ADF, which was described before and shown to most prominently label the subapical actin structure and the least adverse to tube growth compared with several other available plant actin reporters (3–5), transport vesicle reporters, Lat52::GFP-Rab11, and Ch-Rab11, which were as previously described (6) or modified to mCherry (Ch)-tagged, and Golgi body marker, Lat52::GFP-Rab2 (7). For transient tobacco pollen transformation (2–5), 0.8 μg of Lat52:GFP, Lat52::GFP-ADF, 1.5 μg of Lat52::GFP-Rab11, 1 μg of Ch-Rab11 DNA, and 2.5 μg of Lat52::Rab2-GFP were used. For FH5 and derivatives, 0.25 μg of Lat52::FH5, 2 to 2.5 μg of Lat52::FH5-GFP, and 3.5 μg of Lat52:FH5-Ch were used. When used, 2.5 to 5 μg and 10 to 15 μg of FHp::FH5 and FH5p::FH5-GFP DNA, respectively were needed because of the promoter's substantially weaker activity. Five micrograms of Lat52::FH1+FH2 was used. Mock vector DNA was included to equalize input DNA amounts in transient transformation. (*C*) Amino acid sequence alignment between FH5 and available Nt-FH5 sequence. A partial Nt-FH5 cDNA was isolated by RT-PCR from tobacco pollen RNA based on sequence designated as a FH5 homolog described in the Dana-Farber Cancer Institute Gene Index Project http://compbio.dfci.harvard.edu/index.html (TC55287). Amino acid sequence comparison showed the highest homology with FH5 with 72% amino acid identity and 82% similarity spanning the 505 to 747 amino acid region with a single gap, levels substantially higher than with other FHs.

1. Grunt M, Zárský V, Cvrcková F (2008) Roots of angiosperm formins: The evolutionary history of plant FH2 domain-containing proteins. *BMC Evol Biol* 8:115.
2. Twell D, Klein TM, Fromm ME, McCormick S (1989) Transient expression of chimeric genes delivered into pollen by microprojectile bombardment. *Plant Physiol* 91:1270–1274.
3. Chen CY, et al. (2002) The regulation of actin organization by actin-depolymerizing factor in elongating pollen tubes. *Plant Cell* 14:2175–2190.
4. Cheung AY, et al. (2008) The dynamic pollen tube cytoskeleton: Live cell studies using actin-binding and microtubule-binding reporter proteins. *Mol Plant* 1:686–702.
5. Wilsen K, et al. (2006) Imaging the actin cytoskeleton in growing pollen tubes. *Sex Plant Reprod* 19:51–62.
6. de Graaf BH, et al. (2005) Rab11 GTPase-regulated membrane trafficking is crucial for tip-focused pollen tube growth in tobacco. *Plant Cell* 17:2564–2579.
7. Cheung AY, et al. (2002) Rab2 GTPase regulates vesicle trafficking between the endoplasmic reticulum and the Golgi bodies and is important to pollen tube growth. *Plant Cell* 14: 945–962.

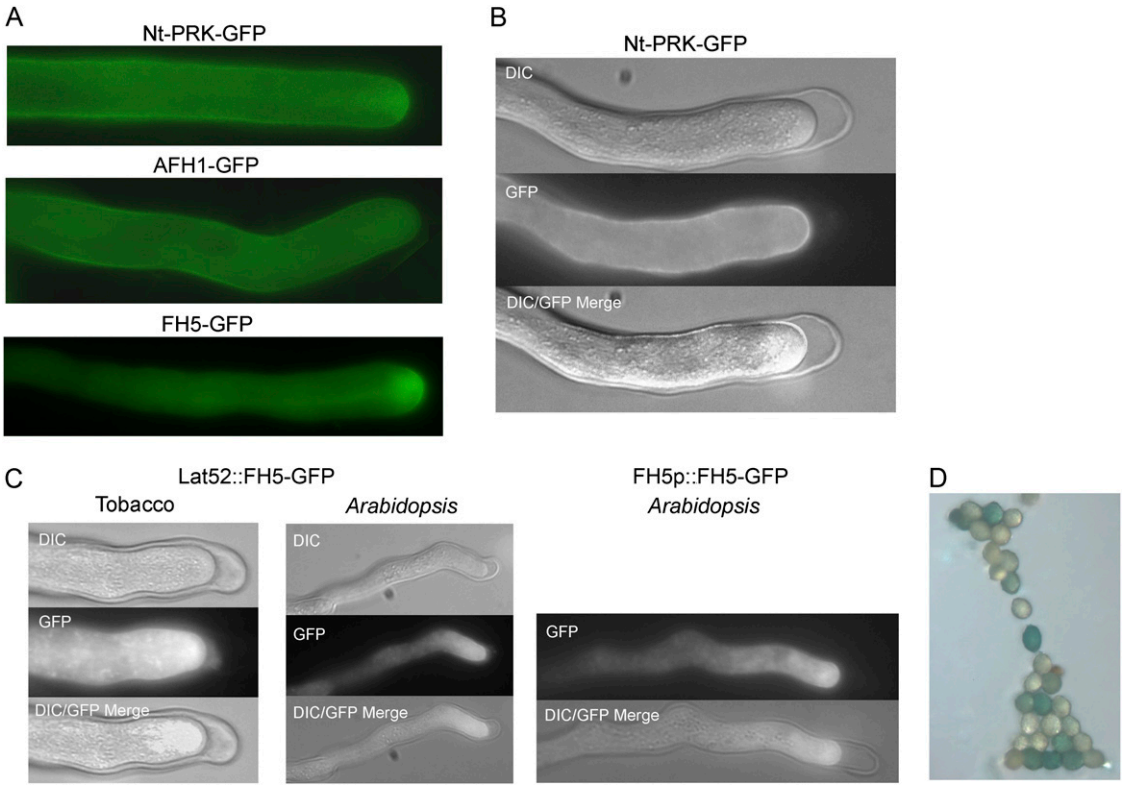

Fig. S2. Comparison of FH5-GFP localization with other pollen-tube cell-membrane protein localization. (*A*) Nt-PRK-GFP (1) and AFH1-GFP (2) localized throughout the pollen-tube cell surface compared with FH5-GFP's apical membrane-associated localization. Pollen receptor kinases (PRKs) from tomato, tobacco, and *Arabidopsis* are well-established pollen-tube cell-membrane proteins (1, 3, 4). AFH1 is a group I formin (5), which as a group is designated membrane-associated because of the presence of a predicated signal peptide, an extracellular domain and a transmembrane domain. Biochemical, immunolocalization and GFP-fusion protein localization studies showed *Arabidopsis* formins 1, 4, 5, 6, and 8 to be cell membrane-located (2, 6–10). (*B*) Plasmolysis of Nt-PRK-GFP transformed pollen tubes. GFP-signal remained associated with the protoplast. (*C*) Plasmolysis of Lat52- or FH5p-expressed FH5-GFP in transiently transformed tobacco and stably transformed *Arabidopsis* pollen tubes. FH5-GFP retained apical prominence and membrane association. Pollen tubes were transformed by 2.5 μg NtPRK-GFP, FH1-GFP, and FH5-GFP. Fifteen-percent mannitol in germination medium was added to pollen-tube growth culture to achieve plasmolysis. Pollen tubes were observed after 2 to 3 min. (*D*) FH5p::GUS expression in transformed *Arabidopsis* pollen: 1 mg/mL of substrate was used under standard GUS reaction conditions (11) for 24 h. Signal was evident but not strong.

1. Cheung AY, et al. (2002) Rab2 GTPase regulates vesicle trafficking between the endoplasmic reticulum and the Golgi bodies and is important to pollen tube growth. *Plant Cell* 14: 945–962.
2. Cheung AY, Wu HM (2004) Overexpression of an *Arabidopsis* formin stimulates supernumerary actin cable formation from pollen tube cell membrane. *Plant Cell* 16:257–269.
3. Muschietti J, Eyal Y, McCormick S (1998) Pollen tube localization implies a role in pollen-pistil interactions for the tomato receptor-like protein kinases LePRK1 and LePRK2. *Plant Cell* 10:319–330.
4. Zhang Y, McCormick S (2007) A distinct mechanism regulating a pollen-specific guanine nucleotide exchange factor for the small GTPase Rop in *Arabidopsis thaliana*. *Proc Natl Acad Sci USA* 104:18830–18835.
5. Grunt M, Zárský V, Cvrcková F (2008) Roots of angiosperm formins: The evolutionary history of plant FH2 domain-containing proteins. *BMC Evol Biol* 8:115.
6. Banno H, Chua NH (2000) Characterization of the *Arabidopsis* formin-like protein AFH1 and its interacting protein. *Plant Cell Physiol* 41:617–626.
7. Yi K, et al. (2005) Cloning and functional characterization of a formin-like protein (AtFH8) from *Arabidopsis*. *Plant Physiol* 138:1071–1082.
8. Deeks M, et al. (2005) *Arabidopsis* group Ie formins localize to specific cell membrane domains, interact with actin-binding proteins and cause defects in cell expansion upon aberrant expression. *New Phytol* 168:529–540.
9. Favery B, et al. (2004) *Arabidopsis* formin AtFH6 is a plasma membrane-associated protein upregulated in giant cells induced by parasitic nematodes. *Plant Cell* 16:2529–2540.
10. Ingouff M, et al. (2005) Plant formin AtFH5 is an evolutionarily conserved actin nucleator involved in cytokinesis. *Nat Cell Biol* 7:374–380.
11. Jefferson RA, Kavanagh TA, Bevan MW (1987) GUS fusions: β-glucuronidase as a sensitive and versatile gene fusion marker in higher plants. *EMBO J* 6:3901–3907.

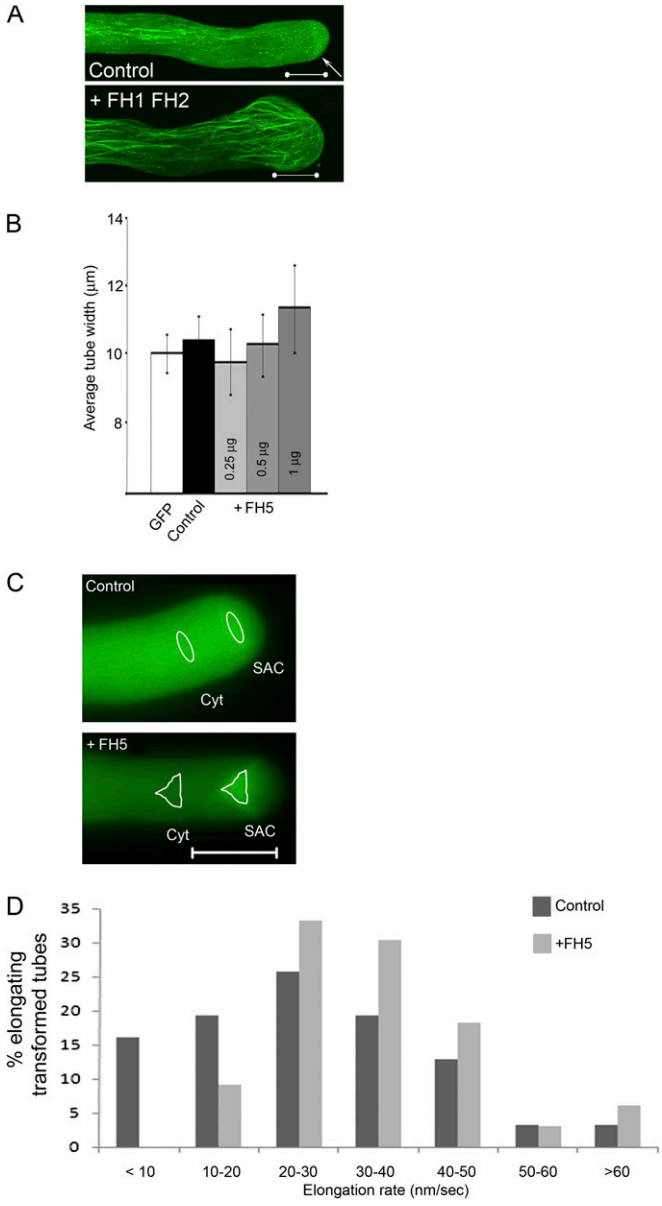

Fig. S3. Supplememtal information on FH5-regulated pollen tube growth. (*A*) The FH1FH2 domains of FH5-induced supernumerary actin cables. Control was transformed by GFP-ADF as actin reporter; the +FH1FH2 tube was cotransformed by FH5 (FH1FH2) (5 μg DNA) and actin reporter. (*B*) Width comparison of pollen tubes from 7-h tubes. Growth correlates negatively with tube diameter allowing pollen-tube width to be used as a measure of pollen-tube growth quality (e.g., refs. 1–3). Student *t*-tests showed differences were significant ($p \sim 10^{-3}$, $\sim 9 \times 10^{-5}$, and $\sim 4 \times 10^{-6}$) for the GFP, the +0.25 μg, and +1 μg samples, respectively, relative to control. (*C*) Quantitative analysis of the relative prominence of the subapical actin structure in control and +FH5 tubes. Average fluorescence intensity for a fixed region of interest (ROI) at the central region of subapical actin structure (SAC) was measured. The intensity level was determined for an identical ROI at the distal cytoplasm (Cyt) between 1- and 2-diameter distance away from the subapical actin structure. The SAC:Cyt ratio was used as a measure of the prominence of the subapical actin structure and equaled to 1.1 and 1.63 for the control and +FH5 tube, respectively, shown here (magnified from Fig. 2*B*). Control SAC:Cyt rarely reached 1.1. A SAC:Cyt = 1.15 correlated strongly with the subapical actin structure being readily noticeable even under wide-field microscopy and clearly discernable from control tubes. We used SAC:Cyt = 1.15 as the base value for the subapical actin structure to be considered as "prominent." The tube-to-tube morphological difference in the subapical actin structure required individually shaped ROI be used for each tube and the SAC:Cyt ratio as a measure for prominence. These calculated ratios correlated with the dramatic difference between the control and +FH5 samples that was readily discerned by direct microscopic observations. (*D*) Pollen-tube growth-rate distribution between controls and +FH5 tubes monitored during elongation. Data were derived from the pollen tubes analyzed in Fig. 2 *G* and *H* ($n = 31$ for controls, 33 for +FH5 tubes). The skewed distribution of +FH5 tubes toward high growth rates underlie the slight but significantly enhanced averaged growth rates in +FH5 tubes shown in Fig. 2*G*. Scale bars, 10 μm.

1. Cheung AY, Wu HM (2004) Overexpression of an *Arabidopsis* formin stimulates supernumerary actin cable formation from pollen tube cell membrane. *Plant Cell* 16:257–269.
2. Zhang Y, McCormick S (2007) A distinct mechanism regulating a pollen-specific guanine nucleotide exchange factor for the small GTPase Rop in *Arabidopsis thaliana*. *Proc Natl Acad Sci USA* 104:18830–18835.
3. Ye Y, et al. (2009) *Arabidopsis* formin3 directs the formation of actin cables and polarized growth in pollen tubes. *Plant Cell* 21:3868–3884.

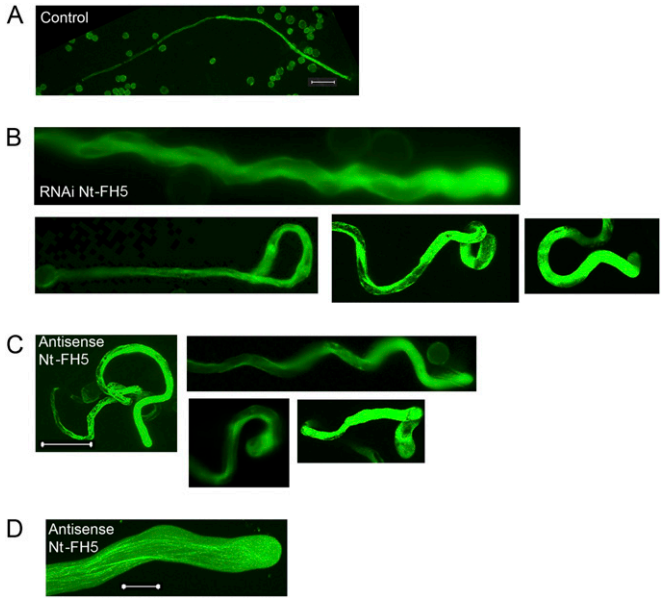

Fig. S4. A control and additional examples of Nt-FH5 RNAi and antisense transiently transformed tobacco pollen tubes. (*A*) A GFP-transformed control pollen tube. (*B*) Other prevalent RNAi Nt-FH5 induced phenotypes. Approximately 80% of the RNAi NtFH5 transformed tubes showed severe meandering (80.3% ± 14%, compared with 2.49% ± 0.75% in control tubes; $n = 3$ independent experiments, each with >50 RNAi Nt-FH5 tubes and between 40 and 55 control tubes); $P \sim 3 \times 10^{-4}$. (*C*) Examples of GFP and antisense Nt-FH5 cotransformed tubes. (*D*) The actin cytoskeleton in an antisense NtFH5 and actin marker cotransformed pollen tube, lacking a pronounced subapical actin structure. Ten micrograms of Lat52::RNAi Nt-FH5 and 15 μg of the Lat52:antisenseNt-FH5 were used in these transformations. Pollen tube morphology was observed after ~10 h of growth; actin cytoskeleton was observed after 6 h of growth. (Scale bars: 50 μm in *A* and *C*; 10 μm in *D*.)

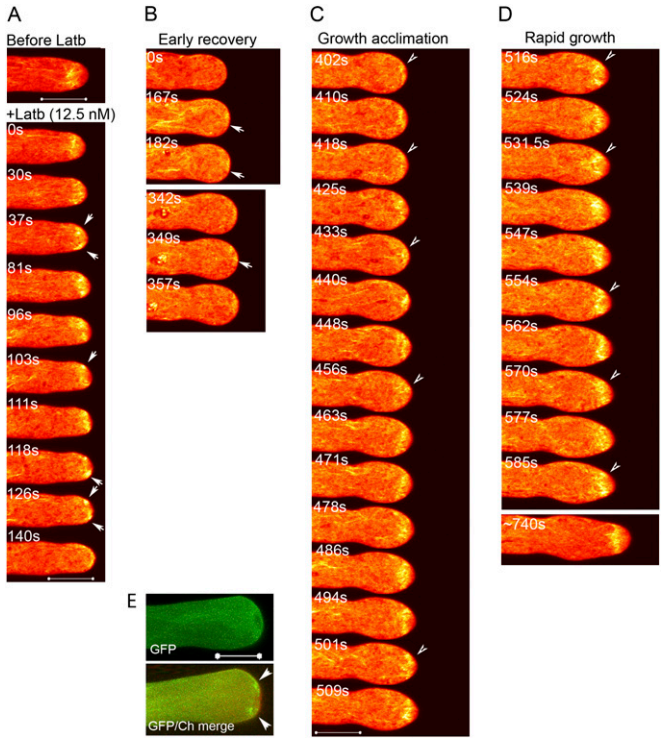

Fig. S5. A comprehensive still-frame presentation of the Latb-treated FH5 transformed pollen tube shown in Fig. 4 monitoring the de novo assembly of the subapical actin reassembly and recovery of tip growth. (*A*) The subapical actin structure before Latb treatment and its dismantling upon addition of Latb. Short arrows and arrowheads in all panels point to subapical actin cables, which typically were the last to disappear in these tubes. (*B–D*) Selected images from the entire growth recovery period (~740 s) starting immediately from Latb washout (0 s). (*B*) Early recovery was accompanied by intermittent emergence of actin filaments from the apical flank membrane. They merged centripetally to form a small actin structure spanning the cytoplasm just distal to the apex (e.g., at 357 s). (*C* and *D*) Growth acclimation and rapid growth began when the assembled actin structure became more persistent. Growth acceleration continued and was accompanied by the reacquisition of a prominent and morphologically dynamic subapical actin structure dynamically and most prevalently maintained at about half the tube diameter's distance from the apex when rapid growth was attained (e.g., from ~500 s onwards, shown in *D*). (*E*) A FH5-Ch and actin marker cotransformed pollen tube recovering from Latb treatment. The whole-tube projection (GFP image) shows an annular configuration of the nascent structure arising at the apical flank. A medial section (GFP/Ch merged image) shows emanation of short actin filaments circumferential to the FH5-Ch localized apical dome. (Scale bars, 10 μm.)

A

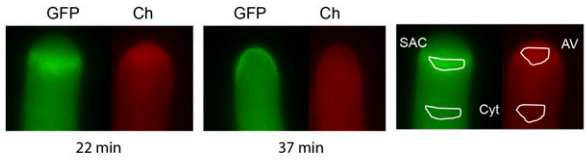

B

Min	0	3	5	8	11	18	22	25	32	35	37
SAC:Cyt	1.42	1.52	1.57	1.54	1.46	1.34	1.52	1.6	1.58	1.3	1.02
AV:Cyt	1.53	1.57	1.67	1.73	1.95	1.61	1.57	1.79	1.26	1.15	1.02

C

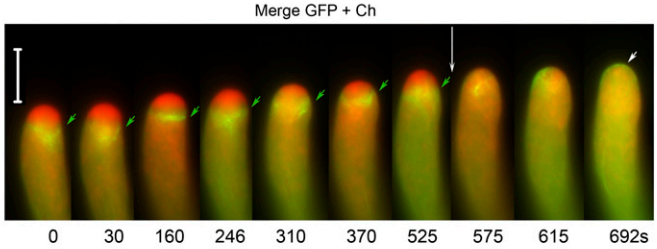

D

Sec	0	30	160	246	310	370	525	575	615	692
SAC:Cyt	1.25	1.5	2	1.99	1.43	1.59	1.4	1.31	1.2	0.96
AV:Cyt	1.9	2.03	2.09	2.12	1.85	1.73	2.07	1.63	1.78	1.23

E

	Rapid growth phase		
Tube #	Average SAC : Cyt	Average AV : Cyt	Average growth rate (nm/sec)
1*	1.47 ± 0.09	1.63 ± 0.17	28.5
2	1.23 ± 0.07	1.58 ± 0.17	24.6
3	1.18 ± 0.03	1.47 ± 0.20	22.3
4*	1.52 ± 0.26	1.88 ± 0.19	23.5
5	1.45 ± 0.12	1.86 ± 0.28	30.5

F

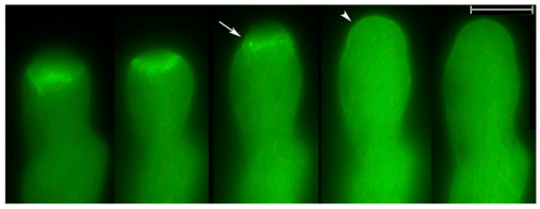

Fig. S6. Analysis details of FH5 induced transition from rapid to decelerated growth in individual pollen tubes. (*A* and *B*) FH5-Ch and actin marker cotransformed pollen tube shown in Fig. 5*A* was analyzed. The 22- and 37-min images are shown (*A*) to illustrate the prominent subapical actin structure and the actin rim, respectively. The SAC:Cyt and FH5-Ch-labeled apical vesicles (AV):Cyt values were analyzed as depicted in *A* and described in Fig. S3C for every time-point shown in *B*. Abrupt drops in both values occurred at the 35- to 37-min transition (*B*) when the average growth rates dropped from 28.5 nm/s to <0.5 nm/s (Fig. 5*A*). (*C*) Time-lapse images of a FH5, actin reporter (GFP-labeled) and vesicle reporter (Ch-labeled) cotransformed pollen tube showing the transition (white arrow) from rapid (0–525 s) to decelerated growth (beyond 525 s) and the concomitant collapse of the subapical actin structure (small green arrows), dissipation of the apical vesicular zone (red), and formation of the apical actin rim (small white arrow). Merged GFP and Ch images are shown; red signals were stretched to make the apical vesicular zone more evident for demonstration. (Scale bar, 10 μm.) (*D*) SAC:Cyt and AV:Cyt values for each time point. Both values dropped abruptly as the apical rim became evident (692 s). The growth rate averaged 23.5 nm/s before the transition and declined to <2 nm/s after apical rim formation. (*E*) Summary data for the average SAC:Cyt and AV:Cyt values during the rapid growth phase of five individual tubes. Tubes one to three were cotransformed by actin reporter (green) and FH5-Ch (red). Tubes four and five were cotransformed by FH5 (unlabeled), actin (green), and vesicle (red) reporter. Tubes one and four (*) are data from the tubes shown in *A* and *C*. Abrupt drops in SAC:Cyt, AV:Cyt and growth rates (to <2 nm/s) in tubes two, three, and five were similar to those shown for tubes one and four. (*F*) Similar observations were made in numerous tubes cotransformed by unlabeled FH5 and actin marker where abrupt disappearance of the subapical actin structure (arrow), formation of an apical actin rim (arrowhead) and growth arrest (between 10 and 13 min for the tube shown here) was coincident. Data from 10 representative tubes showed an average SAC:Cyt of 1.4 ± 0.14 and ~1, respectively before and after the transition to the apical rim stage. Average growth rates dropped from 27.18 + 7.8 to 1.89 ± 1.93 nm/s before and after the transition. (Scale bar, 10 μm.)

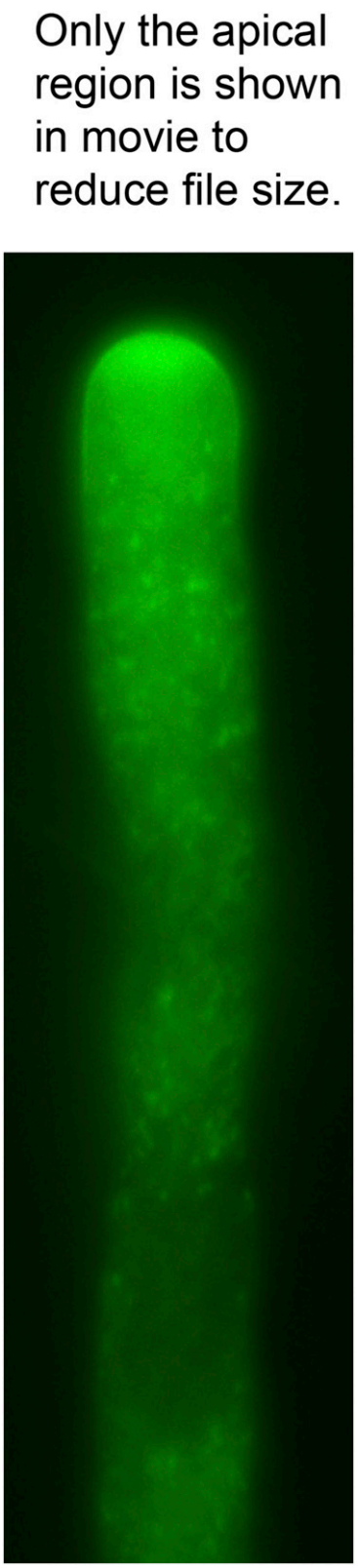

Movie S1. A wide-field time series for an FH5-GFP transformed tobacco pollen tube elongating at ~36 nm/s (~5× accelerated), illustrating the FH5-GFP occupied apical dome membrane, the FH5-GFP–labeled apical vesicular zone, and streaming vesicular congregates in and out of the apical region.

Movie S1

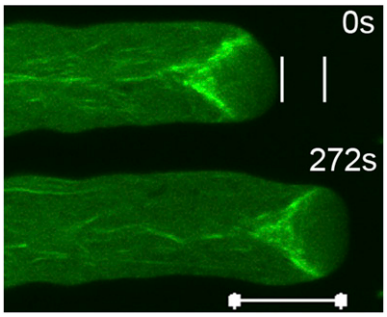

Movie S2. A confocal time series of an actin marker and FH5 coexpressing tobacco pollen tube (shown in Fig. 3*F*) elongating at 26.8 nm/sec (~17× accelerated).

Movie S2

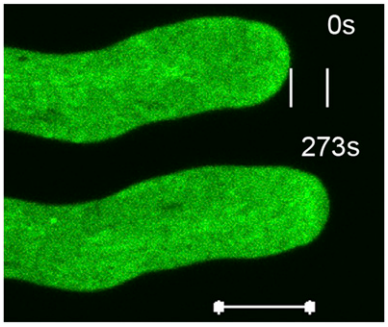

Movie S3. A confocal time series of a control actin marker transformed tobacco pollen tube elongating at 18.9 nm/s and shown >50× accelerated.

Movie S3

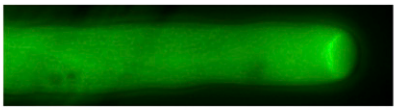

Only the apical region is shown in movie to reduce file size.

Movie S4. A wide-field time series of an FH5 and actin marker cotransformed pollen tube. The pollen tube was elongating at ~21 nm/s. The movie is comprised of 550 continuously acquired images (each at 150-ms exposure) and shown at 1.5× accelerated, and illustrates rapid and continuous morphological changes within millisecond time frames in the pronounced subapical actin structure, not revealed by confocal imaging thus far.

Movie S4

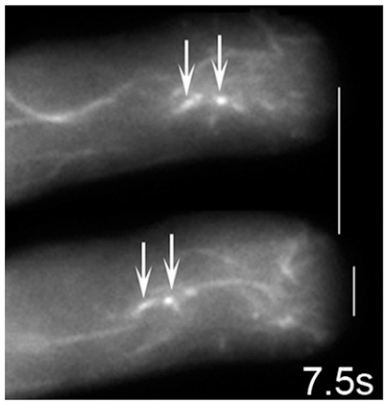

Movie S5. A wide-field time series of an FH5 and actin marker cotransformed tobacco elongating at ~38 nm/s. The movie was made from deconvolved images collected continuously (each at 150-ms exposure) and shown at ~2× accelerated, illustrating rapid reconfiguration within the subapical actin structure and actin retro-flow to join the rearward actin streams in the central cytoplasm.

Movie S5

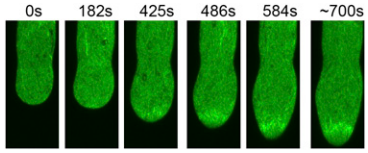

Movie S6. A confocal time series showing the entire recovery process for an FH5 and actin reporter cotransformed tobacco pollen tube after Latb removal (shown in Fig. 4 *A* and *B* and Fig. S5) (~15× accelerated).

Movie S6

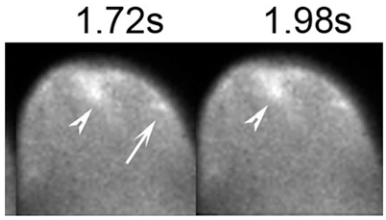

Movie S7. A wide-field time series for an FH5 and actin reporter cotransformed tobacco pollen tube observed at ~5 min after Latb washout (selected images are shown in Fig. 4C). The pollen tube just began to regain growth and was elongating at ~5.8 nm/s and shown at approximately real time. Images were deconvolved to illustrate more clearly dislodging of apical membrane-associated actin to the subapical cytoplasm.

Movie S7

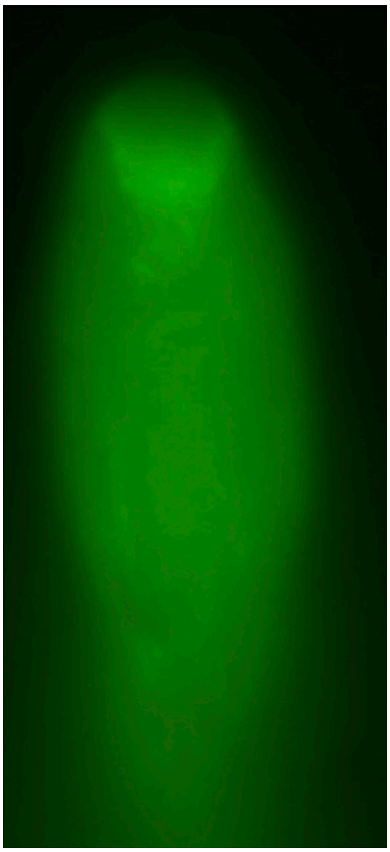

Movie S8. A movie from wide-field time-series images for an FH5 and actin reporter cotransformed tobacco pollen tube observed at ~12 min after Latb washout and shown at ~1.1× accelerated. The pollen tube was regaining growth and elongating at ~8 nm/s. Retroflows of actin from the subapical structure to join the rearward actin streams was evident. The interruption in the movie was from editing of intervening images where medial-plane focus was lost.

Movie S8